J Appl Electrochem (2009) 39:1525–1533
DOI 10.1007/s10800-009-9835-0

ORIGINAL PAPER

Mechanism of boron tribromide electroreduction

Hüseyin Çelikkan · A. Elif Sanli · Hasan Aydin · M. Levent Aksu

Received: 31 January 2008 / Accepted: 9 February 2009 / Published online: 24 February 2009

Abstract This study was carried out to investigate the electrochemical behavior of boron tribromide in dimethlyformamide. The reduction of the compound was found to follow a CE mechanism. The kinetic parameters and the diffusion coefficient were calculated by the use of ultramicrodisc electrodes and chronoamperometry. The number of electrons transferred was found to be 2 by rotating disc and ultramicro disc electrodes and 3 by coulometry. These results are in good accordance with those obtained from molten boron salts. This study is important in regard to electrochemical boronizing at low temperatures.

Keywords Boron · Reduction · Mechanism · Electrokinetics · Deposition

1 Introduction

Boronizing is a process which gives enormous strength to the surface of the substrate to which it is applied. However the process requires elevated temperatures [1]. The coverage of elementary boron on surface is important as regards the semiconductor properties of the resulting coverage. If the substrate is a metal or a metal alloy the boronizing process results in refractory metal borides on the surface [2]. The boronizing process can be carried out thermally [3, 4] or by the electrolysis of molten boron salts [5, 6]. Both these processes take place at elevated temperatures [7]. No studies are reported in relation to low temperature boronizing in the literature.

In the 1950s, the electrochemical behavior of boron halides in different media was investigated [8–11]. Later, Morris et al. published a detailed review of the electrochemistry of boron compounds [12]. Except for these, the literature is rather limited regarding investigation of boron electrochemistry at low temperatures. This study relates to the investigation of the electrochemical behavior BBr_3 on Pt electrodes and boronizing of a st37 stainless steel surface by electrolysis at constant potential.

However, before the boronizing process, the electrochemical properties of precursors such as BBr_3 have to be evaluated. This paper serves this purpose.

2 Materials and methods

2.1 Preparation of the experimental solutions

Boron tribromide is an extremely reactive and toxic compound. It has a very high vapor pressure at room temperature. In order to obviate these harmful effects it is kept in DMF in a less harmful complex form.

Boron tribromide (Merck) and dimethylformamide (Merck) were of 98 and 99.9% purity. The supporting electrolyte was tetrabutylammonium tetrafloride ($TBABF_4$, Aldrich) with 99.9% purity.

The stock solution was freshly prepared with the addition of 0.1 M BBr_3 to DMF solution containing 0.25 M

H. Çelikkan · H. Aydin
Faculty of Science, Department of Chemistry,
Gazi University, Besevler, Ankara, Turkey

A. E. Sanli
Engineering Faculty, Department of Chemical Engineering,
Gazi University, Maltepe, Ankara, Turkey

M. L. Aksu (✉)
Faculty of Education, Department of Chemical Education,
Gazi University, Besevler, Ankara, Turkey
e-mail: maksu@gazi.edu.tr

supporting electrolyte. The experimental concentrations were prepared by the appropriate dilutions of the stock solution.

2.2 Experimental method

All the electrochemical measurements were carried out with CHI 660B electrochemical workstation with BAS C3 cell stand and BAS rotating disc electrode (RDE). The reference and counter electrodes were Ag/Ag^+ (0.01 M $AgNO_3$) with 0.2 M TBATFB/DMF and Pt wire respectively. The working Pt disc electrode (3 mm in diameter) was polished first with 0.5 μm then 0.1 μm alumina and washed with de-ionized water and DMF. The experimental cell was purged with purified argon gas for 10 min prior to the experiments. SEM micrographs were taken with JEOL field emission equipment.

3 Results and discussion

3.1 Electrochemical properties of BBr_3 in DMF

Figure 1 shows the cyclic voltammogram of 1 mM BBr_3 in DMF on the Pt electrode. Two reduction peaks are observed in the cathodic scan located at −0.85 and −1.45 V and there is an anodic peak which appears at −0.8 V in the reverse scan. However, this peak disappears when the scan is reversed at −0.95 V just after the appearance of the first cathodic peak. The fact that the difference between the second reduction peak and the corresponding anodic peak is 650 mV reveals that the electrochemical reduction of BBr_3 in DMF is quasi-reversible.

The current response for the different scan rates is listed in Table 1.

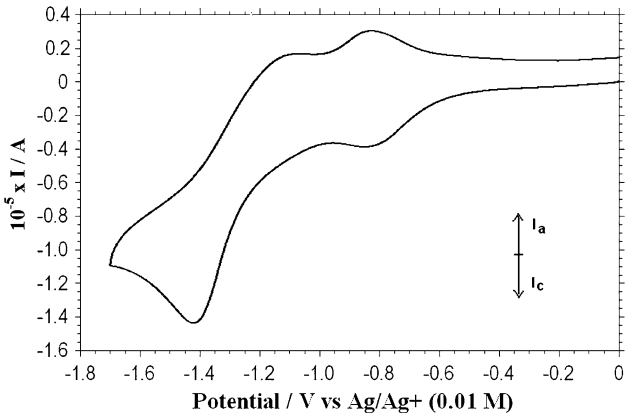

Fig. 1 Cyclic voltammogram of 1 mM BBr_3 in DMF on Pt electrode at a scan rate of 50 mV s^{-1}

The Randles-Ševčik equation is ideal in determining whether the peak observed is diffusion controlled or not. The linearity of a I_p versus $v^{1/2}$ plot is a clear indication of diffusion control.

$$I_p = 2.69 \times 10^5 \, n^{3/2} \, D_0^{1/2} \, C_0 v^{1/2} \quad (1)$$

Figure 2 illustrates the change of $I_p - v^{1/2}$ for the first (−0.85 V) and the second (−1.45 V) cathodic peaks observed for boron tribromide. The R^2 test reveals that the plots are highly linear. The peak observed at −1.45 V is attributable to reduction while it was decided that the peak located at −0.85 V corresponded to adsorption.

Figure 3 shows the corresponding log v–log I_p graphs for the first and second cathodic peaks of BBr_3. The fact that the slopes of the corresponding lines are close to 0.5 indicates that the peaks are diffusion controlled. However the linearity of the peak corresponding to the adsorption process is very low.

Figures 2 and 3 also contain very low scan rates since capacitive current and internal resistance of the solution become much more important at high scan rates.

3.2 Reduction kinetics of BBr_3 in DMF

It is apparent from Figs. 1–3 that the electrochemical behavior of BBr_3 in DMF is quasi-reversible. The plot of anodic to cathodic peak ratio against the scan rate is a useful method in elucidating the underlying mechanism causing this quasi reversible behavior [13] (Fig. 4). The I_{pc}/I_{pa} ratio was observed to increase with scan rate and subsequently level out. Figure 5 shows the change of cathodic and anodic peak currents with scan rate. The cathodic peak current remains constant at scan rates higher than 10 V s^{-1}. It is therefore concluded that BBr_3 gives a chemical reaction before the electrochemical reduction and the product is electrochemically reduced. BBr_3 acts as an acceptor and gives isolated complexes with the ligands containing donor atoms such as nitrogen, oxygen and sulfur [14, 15]. Similarly BBr_3 is thought to give a reaction with DMF solvent molecules as follows:

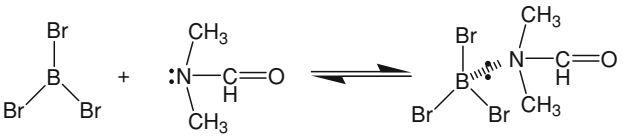

Nicholson and Shain elucidated the relation of current function $I_p/v^{1/2}C_O^*$ and I_{pc}/I_{pa} with the scan rate v [16]. Here C_O^* signifies the bulk concentration. The change in scan rate with current function given in Fig. 6 shows that the reaction follows a C_{rev} E_{rev} (reversible chemical reaction is followed by a reversible electrochemical reaction) mechanism as:

Table 1 The change in two cathodic and corresponding anodic peaks observed in the cyclic voltammogram of BBr_3 at different scan rates

Scan rate (Vs^{-1})	Peak at −0.85 V		Peak at −1.45 V		Reverse Peak at −0.95 V	
	E_p (V)	I_p (A)	E_p (V)	I_p (A)	E_p (V)	I_p (A)
0.01	−0.909	2.50×10^{-7}	−1.423	5.58×10^{-6}	−0.915	4.08×10^{-7}
0.025	−0.858	7.10×10^{-7}	–	–	–	–
0.05	−0.847	1.03×10^{-6}	−1.443	7.14×10^{-6}	−0.827	1.40×10^{-6}
0.075	−0.839	4.80×10^{-7}	−1.431	8.82×10^{-6}	−0.84	2.83×10^{-6}
0.1	−0.848	1.55×10^{-6}	−1.441	1.15×10^{-5}	−0.833	3.20×10^{-6}
0.2	−0.852	2.31×10^{-6}	−1.454	1.52×10^{-5}	−0.808	4.49×10^{-6}
0.5	−0.866	4.40×10^{-6}	−1.486	2.32×10^{-5}	−0.788	8.34×10^{-6}
1	−0.875	4.60×10^{-6}	−1.552	2.63×10^{-5}	−0.738	1.59×10^{-6}
2	−0.886	6.80×10^{-6}	−1.549	4.01×10^{-5}	−0.711	2.93×10^{-6}
5	−0.907	7.00×10^{-6}	−1.599	6.10×10^{-5}	−0.638	5.58×10^{-6}
10	−0.928	7.00×10^{-6}	−1.624	8.26×10^{-5}	−0.625	9.34×10^{-6}
20	–	–	−1.691	8.40×10^{-5}	−0.562	1.52×10^{-6}
50	–	–	−1.758	8.80×10^{-5}	−0.452	2.83×10^{-6}

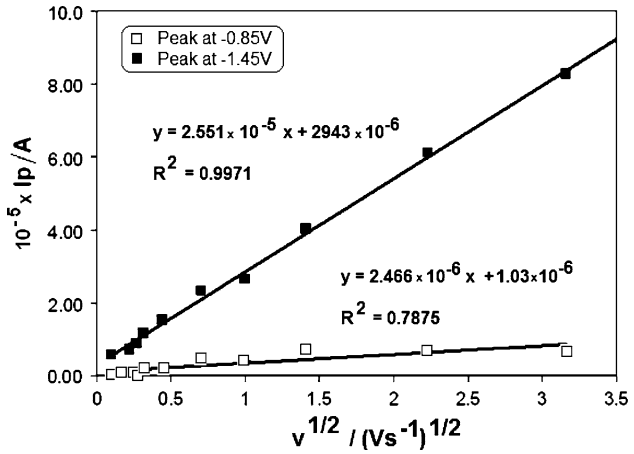

Fig. 2 $I_p/v^{1/2}$ graphs of the first and second cathodic peaks of BBr_3 at different scan rates

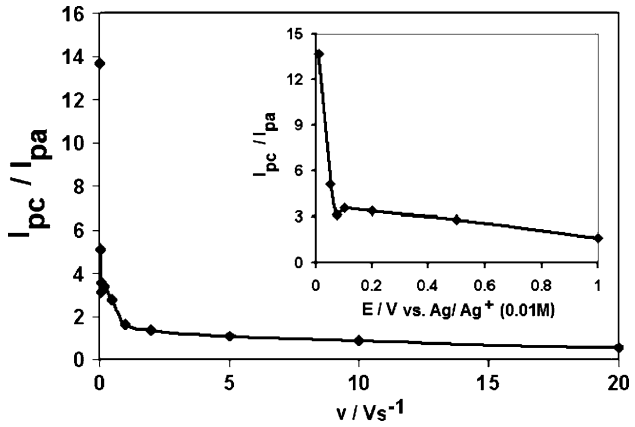

Fig. 4 Change of cathodic to anodic peak current against the scan rate for the two distinctive peaks observed for BBr_3

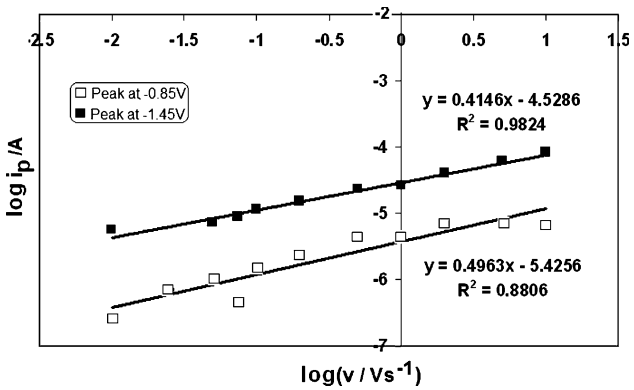

Fig. 3 log I_p–log v graphs of the two distinctive peaks obtained for BBr_3

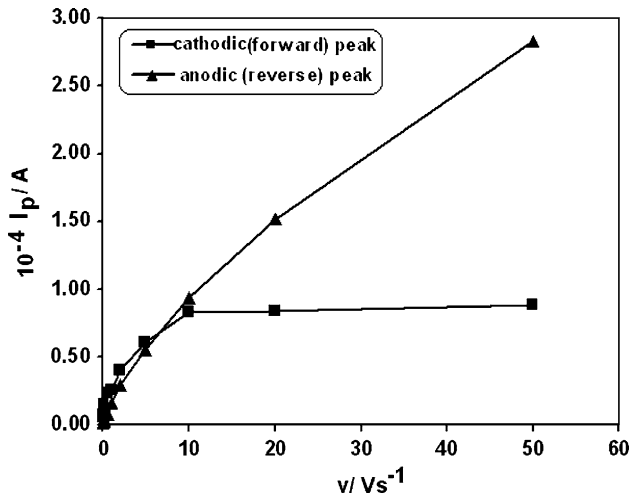

Fig. 5 Change of currents of quasi reversible peaks (−1.85 V cathodic and −0.8 V anodic) against scan rate

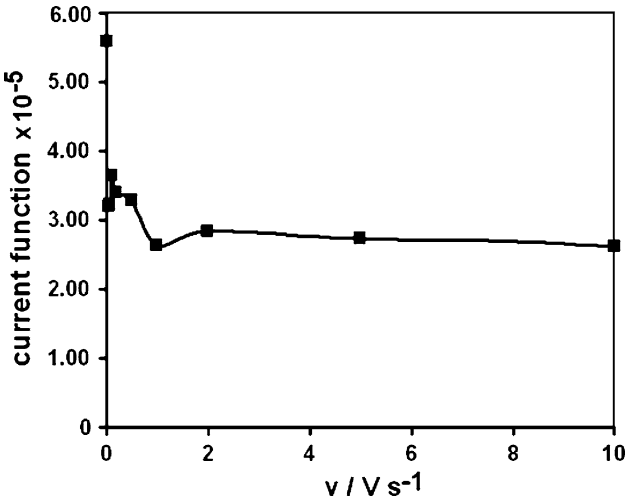

Fig. 6 Current function ($I_p/v^{1/2}$) vs. v graph of BBr_3

$$Z \underset{k_b}{\overset{k_f}{\rightleftharpoons}} Ox$$

$$O + ne \rightleftharpoons R$$

The rates of both the chemical and electrochemical reactions are controlled by the slowest step. The change in peak current with the overpotential ($E_p - E^0$) is given by the Butler–Volmer equation (2) [17]. E^0 for $B^{3+} + 3e \rightarrow B$ is given as −0.789 V (SHE) [18]. This value was found to be −1.142 for the organic medium reference electrode calibrated against ferrocene.

$$I_p = 0.227nFAC_0k^0\left[-\left(\frac{\alpha n_a F}{RT}\right)\right](E_p - E^0) \quad (2)$$

Figure 7 was obtained by the use of Eq. 2. The change of $\ln I_p$ with ($E_p - E_o$) is linear and the slope of the line gives the αn_a value as 0.304 and the intercept gives nk^0 as

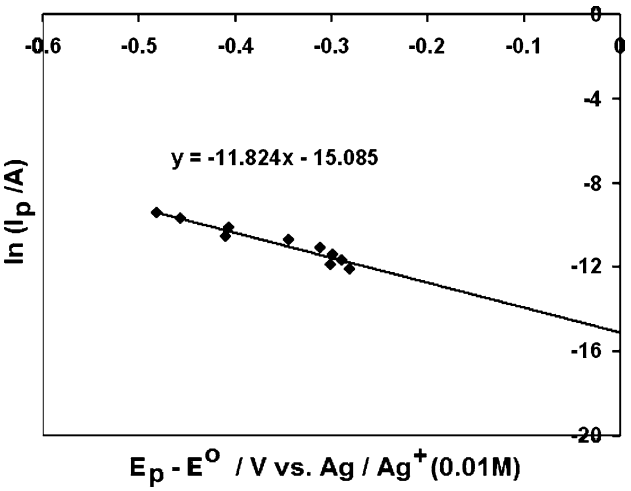

Fig. 7 Graph showing the change of $\ln I_p$ vs. overvoltage (η or E_p–E^o)

1.814×10^{-4}. These values are in good agreement with quasi-reversible behavior.

3.3 Chronocoulometry and chronoamperometry

Chronocoulometry and chronoamperometry are techniques frequently used for the determination of diffusion constants and the number of electrons transferred utilizing the Cottrell (Eq. 3) and the integrated Cottrell (Eq. 4) equations.

$$I = \frac{nFAD_0^{1/2}C_0}{\pi^{1/2}t^{1/2}} \quad (3)$$

$$Q = \frac{2nFAD_0^{1/2}C_0t^{1/2}}{\pi^{1/2}} \quad (4)$$

The graph of I_p against $t^{-1/2}$ and $t^{1/2}$ gives the slopes

$$S = \frac{nFAD_0^{1/2}C_0}{\pi^{1/2}} \quad (5)$$

$$S_p = \frac{2nFAD_0^{1/2}C_0}{\pi^{1/2}} \quad (6)$$

Figure 8 shows the chronocoulometry results obtained for 1 mM Ferrocene and 1 mM BBr_3. The S and S_p values obtained for ferrocene and BBr_3 are 1.39 and 5.86×10^{-5}.

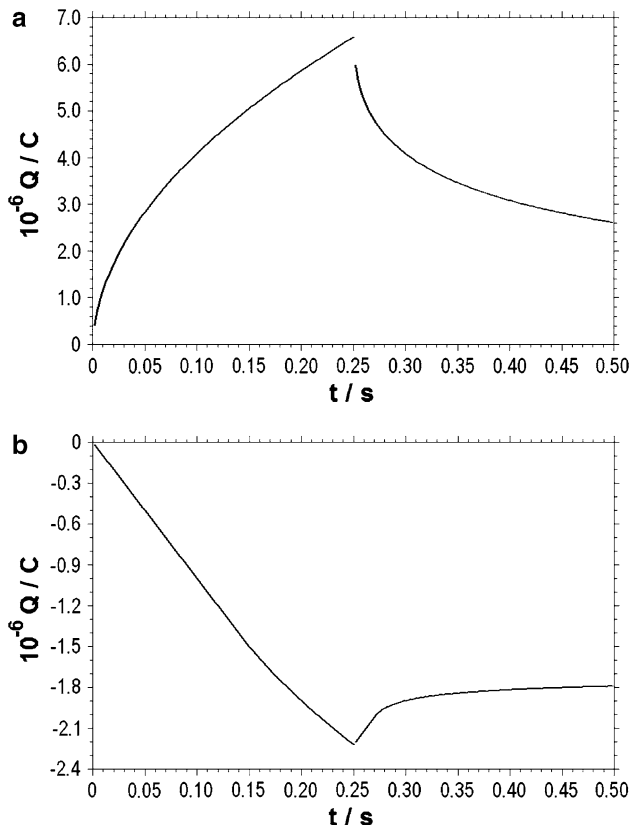

Fig. 8 Chronocoulometric curves obtained for **a** 1 mM BBr_3 and **b** 1 mM Ferrocene

When the S_p value for 1 e transferring ferrocene is substituted in Eq. 2 the area of the Pt electrode and diffusion coefficient D_0 are found to be 0.0707 cm^2 and 3.264×10^{-6} cm^2 s^{-1} .

Ultramicro disc electrodes have very small surface areas which give very small capacitive current during the potential scan. This enables them to be studied at very high scan rates. The steady state current for the ultramicro disc electrode is given as

$$I_{ss} = 4rnFC^0D_0 \tag{7}$$

Figure 9 shows the voltammograms obtained for 1 mM Ferrocene and 1 mM BBr_3 in DMF. The I_{ss} values for ferrocene and BBr_3 are 1.01×10^{-9} A and BBr_3 3.90×10^{-9} A. Equation 8 can be derived from Eqs. 6 and 7. Using the I_p values obtained for ferrocene and BBr_3 the D_0 value for BBr_3 is 1.217×10^{-5} cm^2 s^{-1}.

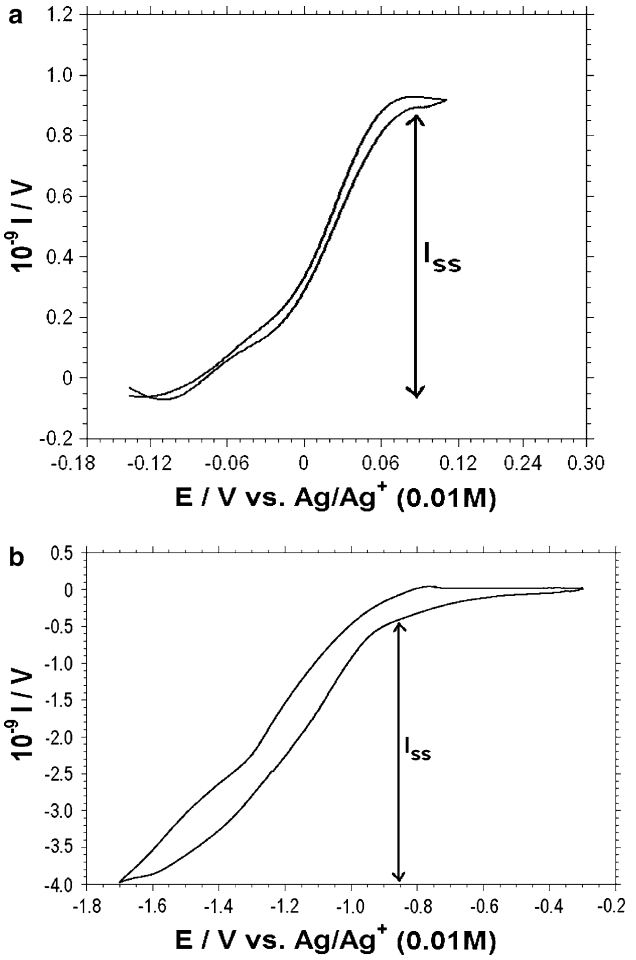

Fig. 9 Ultramicro disc electrode curves obtained with **a** 1 mM ferrocene and **b** 1 mM BBr_3

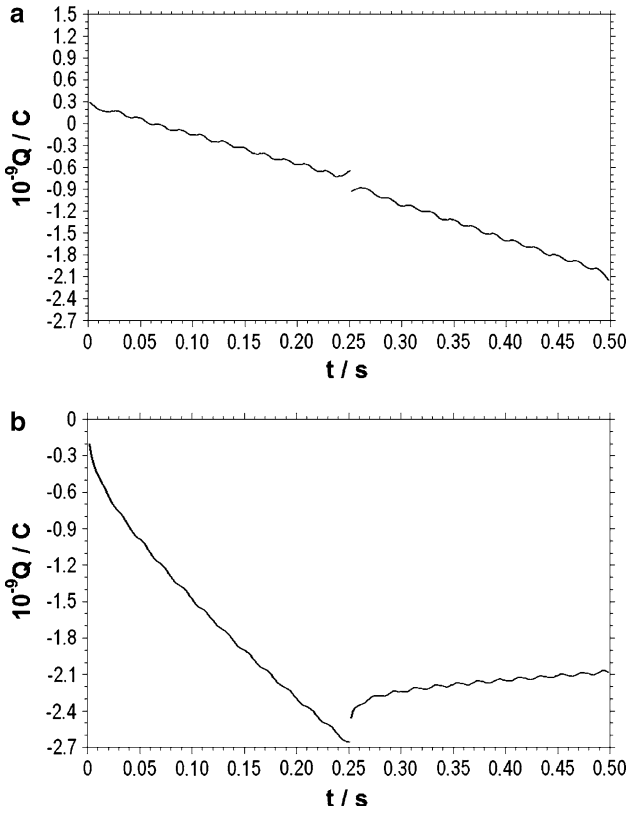

Fig. 10 Ultramicro disc electrode chronocoulometrric curves for **a** 1 mL ferrocene and **b** 1 mL BBr_3

$$\frac{D_0^{1/2}(\mathrm{Fer})}{D_0^{1/2}(\mathrm{BBr_3})} = \frac{I_{ss}(\mathrm{Fer})}{I_{ss}(\mathrm{BBr_3})} \times \frac{S_p(\mathrm{BBr_3})}{S_p(\mathrm{Fer})} \tag{8}$$

This equation can also be employed in the determination of the number of electrons. The number of electrons found in the multi-step reactions is those transferred in the fastest reaction. For this reason the number of electrons transferred, found by the use of ultramicro disc electrodes may not perfectly match those found by coulostatic measurements [19] (Fig. 10).

Using the I_{ss} and D_0 values obtained the number of electrons transferred for BBr_3 is found to be 1.67 by the use of Eq. 7. This value can be approximated to 2. If we take as fact that the number of electrons necessary for BBr_3 is 3 we can conclude that electrochemical reduction takes place in two distinct steps.

3.4 Rotating disc electrode studies

At high rotation rates there are negligible amounts of products and reactants on the electrode surface. The current is given by Levich equation:

$$I = 0.620nF\pi r^2 D_0^{2/3} v^{-1/6} w^{1/2} C_0 \tag{9}$$

Here w and v signify the rotation rate and the kinematic viscosity.

The I–$w^{1/2}$ graph is linear if there is no chemical reaction in the mechanism. Another widely used equation is the Koutecký-Levich equation

$$\frac{1}{I} = \frac{1}{I_k} + \frac{1}{0.620nF\pi r^2 D_0^{2/3} v^{-1/6} w^{1/2} C_0} \quad (10)$$

where I_k is the kinetic current.

The Koutecký-Levich equation is much more useable for w values above 1000 rpm while the Levich equation is more applicable for rotation rates smaller than 1000 rpm when the mechanism contains a chemical reaction step.

Figure 11 contains the RDE data for 1 mM ferrocene and 1 mM BBr_3 in DMF media. Using the D_0 value previously found for ferrocene the kinematic viscosity was found to be 0.0991 $cm^2\ s^{-1}$ at 4000 rpm. Accepting that the kinematic viscosity does not change to an appreciable extent and using the previously found value of the diffusion coefficient, the number of electrons transferred is found to be 1.96, which corresponds well with the ultramicro disc data. This is verification that the reduction of BBr_3 is a two step process. The rate constants were calculated using the following equations:

$$k_f = \frac{I_k}{nFAC^0} \quad (11)$$

$$k_f = k^0 \exp\left(-\frac{\alpha\eta F}{RT}\right) \quad (12)$$

When we substitute the I_k value found from Fig. 11 in Eq. 11 a k_f value of 0.221 is obtained. Using this value together with α and η values previously obtained in Eq. 12 the value of k^0 is found to be 4.027×10^{-4}. This data approximates well with the value obtained from CV data (1.814×10^{-4}).

When we examine Fig. 1, ferrocene gives an ideal plateau shaped curve while BBr_3 gives a peak shaped change. This is an indication that the reduction product is strongly adsorbed on the electrode surface and is not desorbed back into the bulk of the solution.

3.5 Calculation of the amount of BBr_3 adsorbed upon the Pt electrode surface

The peak observed at −0.85 V in Figs. 1 and 2 was attributed to an adsorption process. The relation between the peak current and the amount of substance adsorbed is given by

$$I_P = \frac{n^2F^2}{4RT} vA\Gamma^0 \quad (13)$$

where $\Gamma^0$is the amount of substance adsorbed upon the surface (mol cm^{-3}) .

The slope of the I_p–v graph given in Fig. 12a is 8.201×10^{-6}. If this is substituted in Eq. 13 Γ^0 is found to be 1.372×10^{-11} mol cm^{-3}.

The amount of substance adsorbed on the electrode surface can also be calculated using the coulostatic method. Here the value of the intercept of the forward coulometric response to the charge axis is calculated and the amount of substance adsorbed is determined from

$$Q = \frac{2nFAD_0^{1/2}C^0t^{1/2}}{\pi^{1/2}} + Q_{dl} + nFA\Gamma^0 \quad (14)$$

The value of the intercept was determined from Fig. 12a to be 1.95×10^{-7} C. Neglecting the value for the double

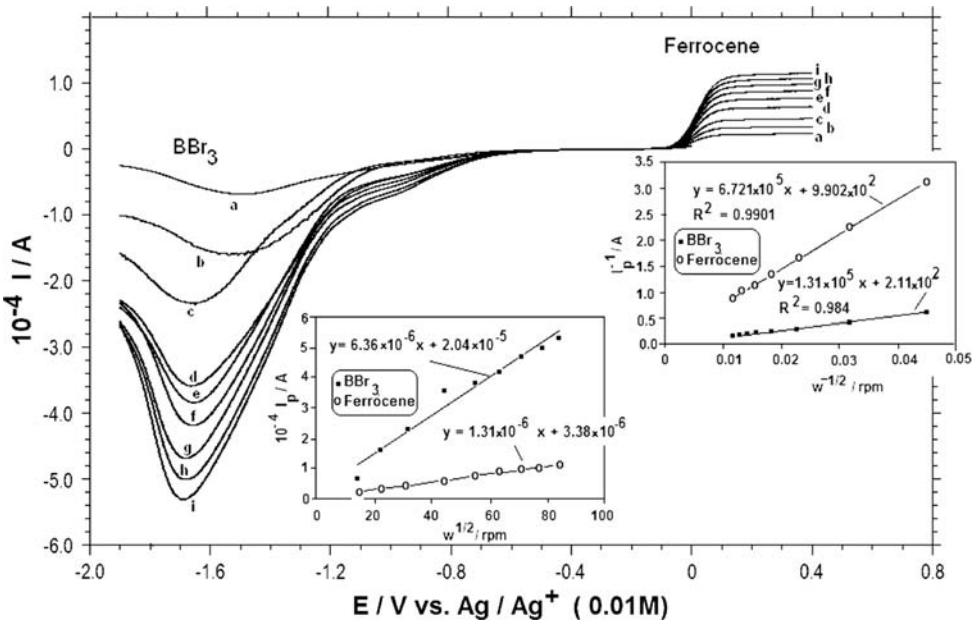

Fig. 11 RDE curves for 1 mM BBr_3 and Ferrocene and related I–$w^{1/2}$ and I^{-1}–$w^{-1/2}$ plots

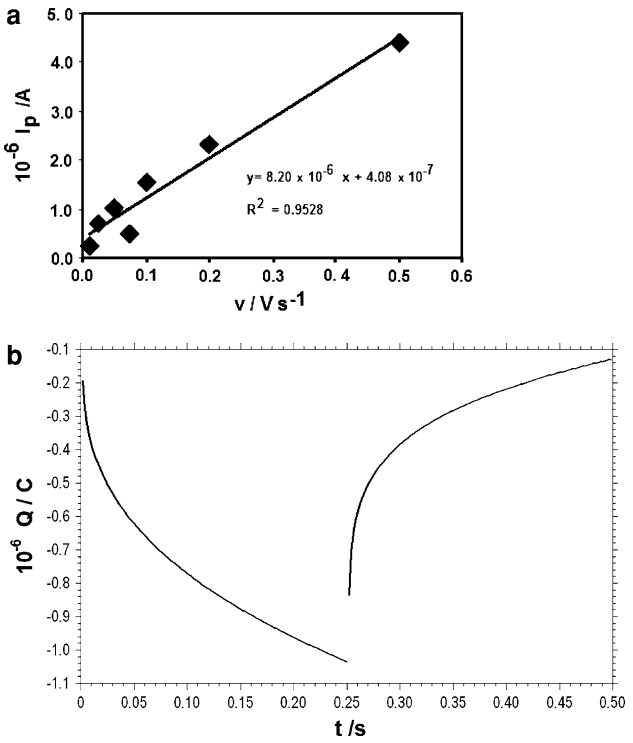

Fig. 12 Calculation of the amount of material adsorbed on the electrode surface by the use of **a** CV and **b** chronocoulometry

layer capacitance Q_{dl} the value of Γ^0 appears as 0.953×10^{-11} mol cm^{-3}. Both the values obtained from CV and coulometry are close to each other.

3.6 Coulometric determination of the number of electrons transferred

As mentioned earlier slow electron transfer makes determination of the number of electrons transferred highly problematic. Bulk electrolysis is an effective and versatile technique in this respect. This method gives the total number of electrons transferred using Faraday's laws. The electrolyses experiments were carried out in a cell separated with a porous disc at a potential of −1.85 V using 11 mL 0.01 M BBr_3 solution in DMF with spiral wire Pt working and Ag/Ag^+ (0.01 M) reference electrodes.

The total charge passed for the exhaustive electrolysis was 35.2 C corresponding to a transfer of 3.32 electrons. This conforms well to the total number of electrons necessary for the electrochemical reduction of BBr_3 (Fig. 13).

3.7 Multi scan voltammetric studies

The multi scan cyclic voltammetric plots are very versatile in the determination of the changes taking place on the electrode surface. Fifty changes were carried out at a scan rate of 50 mV s^{-1} (Fig. 14). The figure shows that the peak

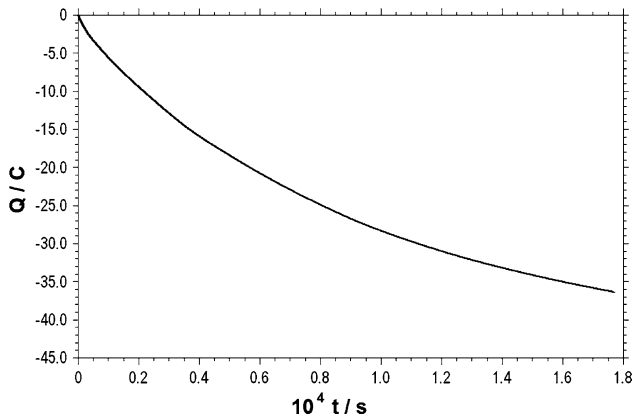

Fig. 13 Coulometric curve of 1 mM BBr_3

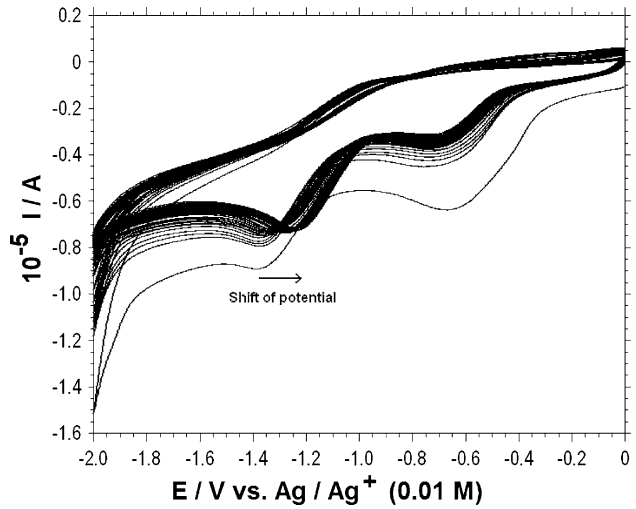

Fig. 14 Multiple sweeps of 1 mM BBr_3 on Pt at a scan rate of 50 mV s^{-1} (50 scans)

at −1.45 V shows an initial decrease before levelling out and shifting positively. The peak at −0.8 V shows a constant decrease. The shift towards positive potentials is particularly important. This shows that the surface is covered with adsorbed product [20]. The surface gradually takes the structure of covered material which makes the coverage easier [21]. This situation manifests itself as a positive shift in potential.

3.8 Boron electrodeposition on the st37 steel

The next step was the boron coverage of st37 steel using BBr_3 in DMF medium. The boron electrodeposition onto the Ti6Al4V alloys was carried out under the same conditions [22]. The boriding of non alloyed st37 is of great industrial importance. 2 cm^2 steel plates were taken and subjected to a cyclic voltammetric scan in 0.01 mM BBr_3 in DMF containing 0.25 M tetrabutyl ammonium tetrafloroborate at a scan rate of 50 mV s^{-1} using a Pt plane

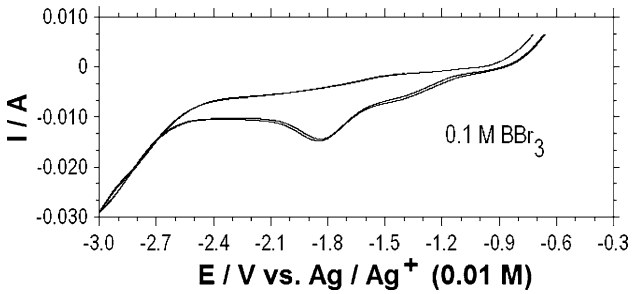

Fig. 15 Cyclic voltammogram for st37 steel electrode in 1 mM BBr_3 solution at 50 mV s^{-1}

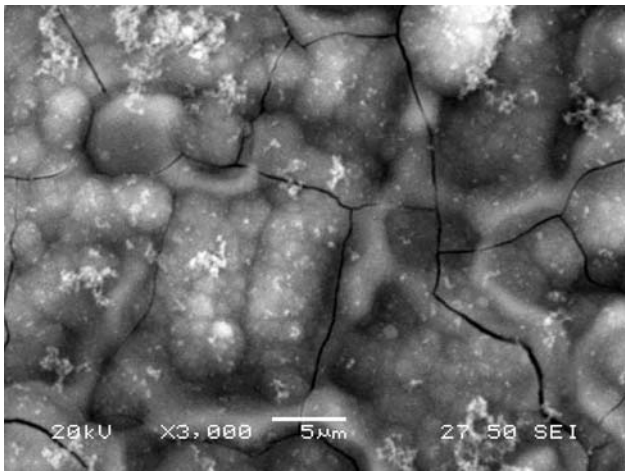

Fig. 16 SEM micrograph of the boron coverage on st37 steel at constant potential using 0.1 M BBr_3 in DMF

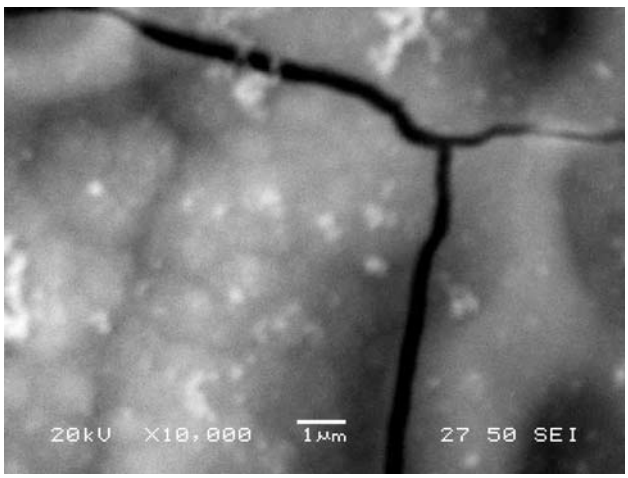

Fig. 17 SEM micrograph of the boron coverage on st37 steel at constant potential using 0.1 M BBr_3 in DMF

counter and organic medium Ag/Ag^+ reference electrode. The resulting voltammogram is depicted in Fig. 15. A reduction peak appears at a potential of −1.85 V corresponding to the reduction of B^{3+} to elementary boron. The solution was electrolysed at a potential of −1.9 V for 12 h. There was a visible and irregular coverage of the surface. The sample was first washed with CH_2Cl_2 and dried at 70 °C under argon for an hour. Figures 16 and 17 show SEM micrographs of the resulting product. The presence of cracks and micro breakages shows that the present conditions are not suitable for providing a protective coverage on the surface.

4 Conclusion

The use of dimethylformamide as a solvent enables BBr_3 to remain in the solution in a complex form. The resulting complex is dissociated during the reduction process but is reformed during the reverse anodic scan in a quasi-reversible manner. The Nicholson and Shain criteria showed that the reduction follows a CE mechanism. The chemical reaction involves the dissociation of the complex followed by the reduction of the BBr_3. The CV, UME and RDE result also support this conclusion.

Although boron coverage was achieved on st37 the presence of cracks and micro ruptures showed that it was not possible to obtain protective boride coverage using this method. It is reported in the literature that amine solvents do not give stabile complexes with BBr_3 but result in the formation of HBr and covalent bonded B–N structures [23, 24]. For that reason the experiments were carried out using freshly prepared BBr_3-DMF complexes. The evolution of hydrogen gas formed by the electrochemical reduction of HBr may cause cracks on the steel surface during the boronizing process using BBr_3.

Acknowledgements The authors are grateful to TUBITAK Research Fund for financial support of this project under Grant No: 106T667.

References

1. Stewart K (1997) Adv Mater Processes 151:23
2. Özbek İ, Bindal C (2002) Surf Coat Tech 154:14–20
3. Petrova RS, Suwattananont N (2005) J Electronic Mater 34:575–582
4. Yang H, Yoshida T (2005) Surf Coat Tech 200:984–987
5. Kaptay G, Kuznetsov SA (1999) Plasmas Ions 2:45–56
6. Li J, Li B (2007) Rare Metals 26:74–78
7. Segers L, Fontana A, Winand R (1991) Electrochim Acta 36:41–47
8. Greenwood NN, Martin RL (1951) J Chem Soc 1795–1798
9. Greenwood NN, Martin RL (1953) J Chem Soc 757–764
10. Greenwood NN, Martin RL (1953) J Chem Soc 751–757
11. Greenwood NN, Martin RL (1953) J Chem Soc 1427–1432
12. Morris JH, Gysling HJ, Reed D (1985) Chem Rev 85:51–76
13. Fey GTK, Hsieh MC, Chang YC (2001) J Power Sources 97:606–609
14. Braunschweig H, Colling M (2001) Coord Chem Rev 223:1–51
15. Shi Q, Li C, Liang YQ (1999) Adv Mater 11:1145–1146

16. Nicholson RS, Shain I (1965) Anal Chem 37:178–190
17. Uçar M, Solak AO, Aksu ML, Toy M (2002) Turk J Chem 26:509–520
18. Pourbaix M (1966) Atlas electrochemical equilibria in aqueous solutions. Pergamon Press, Brussels
19. Lund T, Lund H (1986) Tetrahedron Lett 27:95–98
20. Saidman SB, Quinzani OV (2004) Electrochim Acta 50:127–134
21. Barkey DP (2002) In: Alkire RC, Kolb DM (eds) Advances in electrochemical science and engineering, vol 7. Wiley-VCH, Weinheim
22. Çelikkan H, Öztürk MK, Aydın H, Aksu ML (2007) Thin Solid Films 515:5348–5352
23. Johnson AR (1912) J Phys Chem 16:1
24. Matteson DS (2004) Sci Synth 6:222